THE JOURNAL OF PHYSICAL CHEMISTRY A

ARTICLE

pubs.acs.org/JPCA

N, P, and As Ylides and Aza- and Arsa-Wittig Reactions from Topological Analyses of Electron Density

Ángel Sánchez-González,[†] Santiago Melchor,[†] José A. Dobado,*[,†] Bernard Silvi,[‡] and Juan Andrés[§]

[†]Grupo de Modelización y Diseño Molecular, Departamento de Química Orgánica, Universidad de Granada, 18071-Granada, Spain

[‡]Laboratoire de Chimie Théorique (UMR-CNRS 7616), Université Pierre et Marie Curie, 4 place Jussieu, 75252 Paris, France

[§]Departament de Química Física i Analítica, Universitat Jaume I, 12071 Castello de la Plana, Spain

Supporting Information

ABSTRACT: The nature of bonding between N, P, and As constituent atoms in ylide systems with the R_3XYR' formula (X = N, P, As; Y = N, P, As; R = F, H; R′ = H, CH_3) has been characterized by ab initio (MP2/6-311++G**) and density functional theory (B3LYP/6-311++G**) calculations. Its electronic structure has been analyzed through electron density with the quantum theory of atoms in molecules and the electron localization function (ELF). The characteristics of the central bond are inspected with the calculated rotational barriers. The results show that N has a behavior different from that of the remaining pnicogen atoms (P, As), where the bond is much stronger. Fluorine substituents strengthen the X−Y bond, reduce the bond distance, and increase the electron density in the central bond so that the substituent pulls charge from the bond in the pnicogen X atom. For the N−pnicogen ylides, the results showed different bonding characters between F and X atoms; depending on the position of the F atom, the difference of the bond character is sensed by the basin synaptic order, as it is deduced from the analysis of the ELF basins. The energy profiles of the rotational barriers have been calculated at the MP2/6-311++G** level, indicating that the electronegativity of the substituents is a relevant factor that has consequences in the characteristics of the X−Y bond.

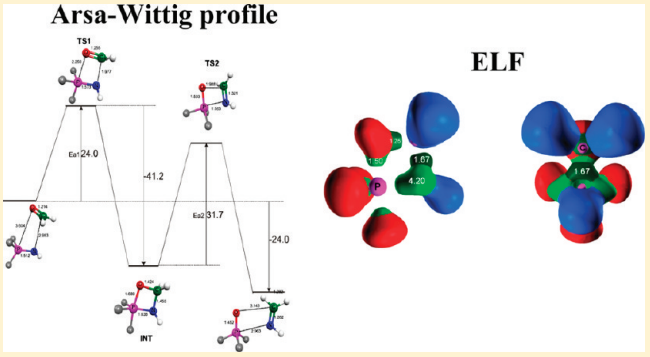

1. INTRODUCTION

Molecules that have a contributing Lewis structure with opposite formal charges in adjacent atoms are defined as ylides. These sorts of molecules have been demonstrated to be useful in organic chemistry for the synthesis of highly functionalized compounds. In particular, ylides are suitable for the construction of double bonds between carbon and pnicogen atoms (X = N, P, and As) through Wittig-analogue reactions, such as the aza-Wittig[1,2] and arsa-Wittig[3−6] reactions, providing C═N and C═As double bonds, respectively. The ylides studied are listed in Scheme 1 for evaluating the behavior of the central bond and their corresponding chemical reactivity. Scheme 2 illustrates how the zwitterionic character of the bond in the ylides results in an alignment with the C═O bond of molecules containing a keto group; therefore, their chemical reactivity is controlled by the formation of a complex characterized by a four-membered central ring that results in the cleavage of the C═O and P−N/As bonds and formation of the N/As═C and P═O bonds.

Although iminophosphoranes (R_3P−NR) have been extensively studied,[7] the characterization of the bonding nature is still a challenge. Different interpretations of their nature persist: some authors, from geometrical data and MO analysis, suggest a partial triple bond,[8] while others[9−11] give more relevance to the zwitterionic character of H_3P−NH on the basis of geometrical data, MO analysis, charges, and other properties such as its basicity.

Another ylide pnicogen analogue, iminoammonium (H_3N−NH), has also been investigated[8,11] where ylidic character is assigned. However, a general study on their reactivity and characterization of the bonding nature is missing in the literature. Similarly, the phosphinophosphorane derivatives have been widely studied,[12,13] but with avoidance of an explanation on the bond character in this ylide. Finally, arsenic ylides used in arsa-Wittig reactions[5] have not yet been studied theoretically, and their bonding nature has not been reported.

All the above-mentioned works agree that the pnicogen−pnicogen ylides are stable structures regarding their respective tautomeric forms derived from energy-barrier calculations, but generally, the bonding nature and the role of substituents for these bonds have not been previously discussed in terms of the quantum theory of atoms in molecules (QTAIM)[14−16] or electron localization function (ELF).[17−20]

Received: May 12, 2011
Revised: June 20, 2011
Published: July 07, 2011

Scheme 1. Geometries for Pnicogen−Pnicogen Compounds 1a−d to 9a−d of the Studied Ylides

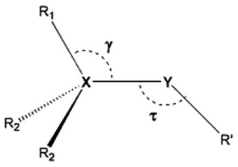

	X	R = R' = H	R = F, R' = H	R = H, R' = Me	R = F, R' = Me
Y = N	N	1a	1b	1c	1d
	P	2a	1b	2c	2d
	As	3a	3b	3c	3d
Y = P	N	4a	4b	4c	4d
	P	5a	5b	5c	5d
	As	6a	6b	6c	6d
Y = As	N	7a	7b	7c	7d
	P	8a	8b	8c	8d
	As	9a	9b	9c	9d

Scheme 2. General Scheme for Aza- and Arsa-Wittig Reactions, Top and Bottom, Respectively

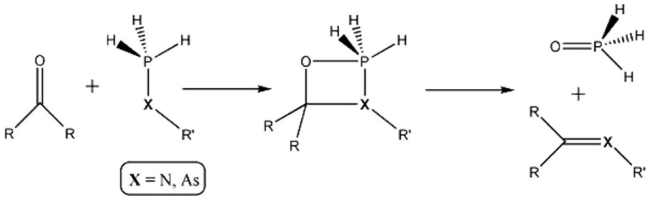

The aza-Wittig reaction has been demonstrated as a powerful tool for constructing C═N double bonds in organic synthesis.[21] On the basis of a theoretical study, Cossío et al.[22] conclude that the reaction corresponds to a formal [2 + 2] cycloaddition. Xue et al.[23] gave structural information on the different steps involved in the reaction together with thermodynamic and kinetic properties. The characteristics of the bond in iminopnictoranes and its behavior in the aza-Wittig reactions have been described by Koketsu et al.,[24] reporting a zwitterionic bond in N−pnicogen ylides, although the double-bond character is explained by negative hyperconjugation. Moreover, two conformers for the cyclic intermediate are reported. Other authors[23,25,26] have made a theoretical study of the aza-Wittig reaction but have reported only geometrical data and energetic barriers. However, the arsa-Wittig reaction[3−6] is a useful organic reaction for constructing C═As double bonds and in olefination chemistry because of its high stereoselectivity and the mild reaction conditions used,[27] for which no theoretical data have been reported.

The goal of this work is to gain deeper insight into the bonding characteristics of these compounds and to relate this to the chemical reactivity involved in the aza- and arsa-Wittig reactions. To this end, the topology of the electron density displayed by both the QTAIM and the ELF procedures has been analyzed in detail.

2. METHODOLOGY

Ab initio and density functional theory (DFT) calculations, at the Møller−Plesset[28] second-order-corrected (MP2) and Becke three-parameter Lee−Yang−Parr (B3LYP)[29] theoretical levels, respectively, have been performed with the 6-311++G** basis set for the pnicogen−pnicogen ylides studied using the Gaussian03 program.[30] All structures were fully optimized at the above-mentioned MP2/6-311++G**//MP2/6-311++G** and B3LYP/6-311++G**//B3LYP/6-311++G** theoretical levels. The nature of stationary points on the potential energy surfaces was confirmed by calculating the eigenvalues of the matrix of second derivatives (Hessian); none of the energetic minima presented any imaginary frequencies, while transition states (TSs) presented a single imaginary frequency.

The bonding scheme present in these compounds was studied with the QTAIM[14−16] and ELF[17−20] methodologies. In QTAIM theory, the topological analysis of the electron density provides an accurate definition of the chemical concepts of the atom, bond, and structure, as pointed out by Bader.[14−16] This theory allows the partition of the molecular space into separate regions associated with atoms, and thus, an atom in a molecule is defined as the region of the space delimited by zero flux surfaces. For each point contained in the atomic basin, the gradient paths of the electron density lead to the atomic center with which the basin is associated. From the previous definition, the concept of a bond between two atoms arises naturally: within a molecular system at equilibrium, two atoms are said to be bonded when they share a common interatomic surface (the zero-flux surface) through which they can interact, this being a common boundary condition for the independent resolution of the Schrödinger equation for each basin. This is the reason why atomic basins are also referred to as "open systems". This bonding condition is satisfied when there is a point (contained in the zero-flux surface) where the electron density is a minimum in a specific direction in space but a maximum in the plane perpendicular to it. These points are known as bond critical points (BCPs), and the pair of gradient paths that connect the BCPs with each nucleus is referred to as the atomic interaction line or bond path. With respect to the ELF function, this was first introduced by Becke and Edgecombe[17] and reinterpreted by Silvi and Savin[18] as a measure of the excess of local kinetic energy due to Pauli's exclusion principle, in comparison to a uniform electron gas. The ELF, as defined in the literature,[18−20] is a function that yields values between 0 and 1. Values close to 1 indicate electron pairing at that point, whereas values near 0 are usually found in regions between electron pairs. As in QTAIM analysis, it is possible to divide the molecular domain into basins grouped around the ELF attractors. From a chemical standpoint, basins can be classified as being core, valence, or hydrogenated. When the basin does not contain a nucleus, it is called a valence basin, whereas when it contains a nucleus other than a proton, it is called a core basin. It is called hydrogenated when a proton is inside the basin. Valence basins are characterized by the number of core basins with which they are connected, this being known as the synaptic order.[31] Thus, it provides valuable information on the location, size, population, and multiplicity of bonds and, most important, the degree of bond-character reduction in situations where bond connectivity is not clear. QTAIM data at the BCPs were calculated with MORPHY98,[32−34] while charges were integrated with AIM2000 software.[35] ELF was computed with ToPMoD,[31] and isosurfaces were rendered with the SciAn[36] visualization package.

The ELF plots consist of the ELF isosurfaces at a fixed value of 0.7. The color convention represents core basins in magenta, and the colors of the remaining valence basins depend on their synaptic order,[37] red, green, and cyan for monosynaptic, disynaptic, and hydrogenated basins, respectively.

Rotational barriers were calculated for all the compounds at the MP2/6-311++G**//MP2/6-311++G** level, starting from the optimized minimum structure and modifying the R−X−Y−R′ dihedral angle, where R and R′ are those atoms lying on the symmetry plane, the other geometric parameters

dx.doi.org/10.1021/jp204441p |J. Phys. Chem. A 2011, 115, 8316–8326

Table 1. Geometrical Parameters for Compounds 1a,b−9a,b, X−Y, R_1−X, R_2−X, and Y−R′ Bond Distances and Angles τ and γ, Calculated at the MP2/6-311++G//MP2/6-311++G** Level**

		X−Y (Å)	R_1−X (Å)	R_2−X (Å)	Y−R′ (Å)	τ (deg)	γ (deg)
1a	H_3N−NH	1.457	1.019	1.029	1.024	101.8	105.1
2a	H_3P−NH	1.570	1.393	1.417	1.015	115.2	109.0
3a	H_3As−NH	1.718	1.488	1.516	1.024	108.4	107.6
4a	H_3N−PH	1.946	1.018	1.017	1.415	88.4	107.4
5a	H_3P−PH	2.088	1.396	1.408	1.416	87.7	109.3
6a	H_3As−PH	2.200	1.492	1.507	1.417	87.9	110.1
7a	H_3N−AsH	2.105	1.017	1.016	1.519	87.2	107.8
8a	H_3P−AsH	2.232	1.397	1.406	1.519	88.4	109.1
9a	H_3As−AsH	2.339	1.494	1.506	1.521	87.3	110.3
1b	F_3N−NH	1.210	1.352	1.546	1.023	109.0	116.2
2b	F_3P−NH	1.505	1.552	1.569	1.007	125.1	111.2
3b	F_3As−NH	1.662	1.699	1.725	1.024	110.3	110.0
4b	F_3N−PH	1.700	1.789	1.365	1.409	88.4	118.0
				1.355[a]			
5b	F_3P−PH	2.003	1.564	1.577	1.420	82.5	113.5
6b	F_3As−PH	2.124	1.715	1.731	1.423	82.4	114.6
7b	F_3N−AsH	1.845	1.829	1.356	1.512	87.7	116.2
				1.359[a]			
8b	F_3P−AsH	2.145	1.566	1.577	1.523	82.9	113.0
9b	F_3As−AsH	2.259	1.718	1.732	1.526	81.5	114.7

[a] Different distance for R_2 substituent in compounds without C_s symmetry.

Table 2. Standard Bond Distances (Å) Calculated at the MP2/6-311++G//MP2/6-311++G** Level**

	single	double
NN	1.472	1.258
PN	1.719	1.602
PP	2.237	2.040
AsAs	2.473	2.281
AsN	1.867	1.737
AsP	2.357	2.161

being frozen during the scan to preserve the electronic environment near the pnicongen atom.

3. RESULTS AND DISCUSSION

3.1. Pnicogen Ylides. *3.1.1. Geometry.* First, we describe the geometrical results from the theoretical calculations for the compounds studied with the molecular formula R_3XYR'. Table 1 summarizes the geometrical parameters calculated at the MP2/6-311++G**//MP2/6-311++G** level for those compounds where R′ = H (**a** and **b** series). The remaining methylated compounds are listed in the Supporting Information. In addition, Table 2 lists the values calculated for the single and double pnicogen−pnicogen bonds. All compounds showed C_s symmetry except for N−P and N−As ylides, where the N atom has fluorine substituents.

Scheme 3. Geometrical Scheme for Ylides where F Is Connected to the N Atom in the X Position, 4b, 7b, 4d, and 7d

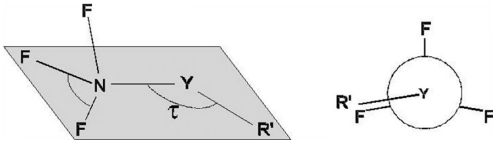

The general trend observed is the reduction of the X−Y bond distance between pnicogen atoms when compared to the corresponding pnicogen−pnicogen single bonds (see Table 2). This behavior can be explained by the electrostatic contribution to the bond shortening due to the opposite charges in central atoms.

Only compounds **4a** and **7a**, with N−P and N−As, show an increment of the bond length values, while the rest of the compounds show a short distance and bring the bonds closer to double-bond values. Moreover, for compounds **2a** and **3a**, the central bond length is shorter. This suggests that the shortening of these X−Y bonds may present a higher bond order that approaches a double-bond character. This behavior will be examined in detail below with the ELF and QTAIM analyses.

If the X atom presents fluorine as a substituent (comparing **a** and **b**), the X−Y distance is reduced for all compounds, but notably, in the N−pnicogen ylides, the bond distance shows the largest reduction for several compounds (0.247 Å from **1a** to **1b**, 0.246 Å from **4a** to **4b**, and 0.260 Å from **7a** to **7b**) while the remaining variations are kept below 0.08 Å. This selective bond-length decrease indicates a substantial change in bond multiplicity induced by fluorine. This effect can be sensed along the series (**c** and **d** behave similarly; see Table S-1 in the Supporting Information).

Such a noticeable bond reduction in nitrogen ylides **1a**, **4a**, and **7a** contrast sharply with the remaining compounds and matches a distinct bonding arrangement in nitrogen ylides. The other compounds, even after F substitution, showed bond lengths similar to those of the prototypical double bonds, while **1a**, **4a**, and **7a** did not. Therefore, this could mean that the ylidic character for **1a**, **4a**, and **7a** has been replaced by a double bond, although this requires confirmation from the topological analysis of the electron density.

Regarding the R−X bond distances, we sensed that a substituent located at the symmetry plane is invariably closer to the pnicogen atom, except for **1a**, **4a**, and **7a**, corresponding to H_3N−NH, H_3N−PH, and H_3N−AsH compounds, respectively. This agrees with single X−Y bond character, contrary to the ylidene form. However, when the R substituent is fluorine, a special situation arises: **4b**, **7b**, **4d**, and **7d** lose their previous symmetry. In these compounds, F substantially alters the molecular structure, two F atoms appearing, with X, Y, and R′ arranged approximately in a plane and the remaining F atom being placed clearly outside this plane far away from the N in the X position (1.7−1.8 Å) (see Scheme 3). Additionally, for compounds **1b** and **1d**, the symmetry remains despite the fact that different bond lengths between the R substituents appear. We see clearly how the fluorine effects are most dramatic for the compound containing N at the X position.

The values of the τ angle are dependent on the particular pnicogen combination at the central X−Y bond. For the **a** series, generally τ is less than 90°. However, when Y = N (**1a**−**3a**), the angles proved to be far above 100°, compound **2a** yielding the largest τ angle, 115°. This behavior, incompatible with the classic

Table 3. Electronic Properties for X−Y Bonds in Compounds 1a−d to 9a−d, Electron Density at the Bond Critical Point, Its Laplacian, Ellipticity, and Electronic Energy Density, Delocalization Index between the X and Y Basins, and Total Charges Integrated over the X and Y Basins, q_X and q_Y, Computed at the B3LYP/6-311++G//B3LYP/6-311++G** Level**

		$\rho(r_c)$ (e^- a_0^{-3})	$\nabla^2\rho(r_c)$ (e^- a_0^{-5})	ε	$E_d(r_c)$ (hartrees a_0^{-3})	δ(X,Y)	q_X (e^-)	q_Y (e^-)
1a	H_3N-NH	0.259	−0.201	0.194	−0.207	1.16	−0.80	−0.79
2a	H_3P-NH	0.210	0.694	0.160	−0.188	0.98	3.03	−1.69
3a	H_3As-NH	0.188	0.131	0.139	−0.139	2.56	1.84	−1.28
4a	H_3N-PH	0.089	0.040	0.722	−0.055	0.7	−1.23	0.50
5a	H_3P-PH	0.118	−0.134	0.634	−0.085	1.12	1.78	0.44
6a	H_3As-PH	0.101	−0.073	0.496	−0.053	2.32	1.12	−0.32
7a	H_3N-AsH	0.074	0.154	0.244	−0.020	1.34	−1.2	0.31
8a	H_3P-AsH	0.096	0.035	0.398	−0.042	1.24	1.82	0.21
9a	$H_3As-AsH$	0.083	0.033	0.428	−0.031	2.18	1.08	0.19

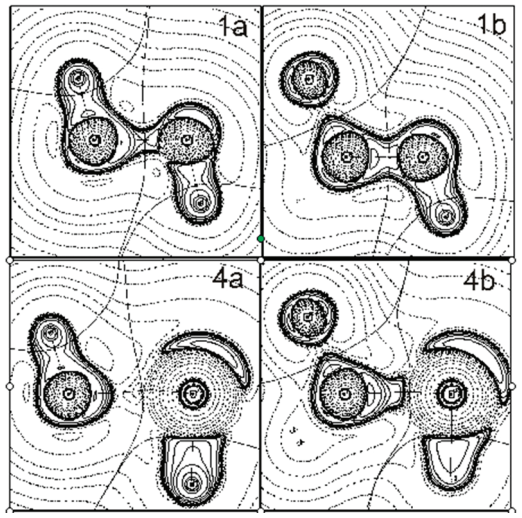

Figure 1. Laplacian plot of the electron density for compounds **1a,b** and **4a,b**. The $\nabla^2\rho(r)$ contours begin at zero and increase (dashed contours) and decrease (solid contours) in steps of ±0.02, ±0.04, ±0.08, ±0.2, ±0.4, ±0.8, ±2.0, ±4.0, and ±8.0. The thick lines represent the atomic interaction lines joining the nuclei, solid squares represent the BCP, and solid triangles represent the ring critical point.

Lewis interpretation, can be explained only with the ELF analysis in terms of the electron density (see below). This trend is also valid for the remaining series, although series **d** presents higher values (τ angles up to 146.5°) due to the combination of both electronic and steric effects.

With respect to the γ angle values, the effect of F substitution is low, although an increase of the corresponding value can be sensed. This behavior can be associated with a larger value of the electron density on the central region of the molecule.

3.1.2. QTAIM Analysis. The central X−Y bonds of these pnicogen−pnicogen ylides were analyzed using the QTAIM theory. In Table 3, the corresponding values for the BCPs are presented. The electron density, $\rho(r)$, marks the bond strength and partially indicates the population located between two bonded atoms, while the electron energy density indicates the stabilization due to the presence of the bond.

Overall, a clear distinction between **1a**−**3a** and **4a**−**9a** can be found in both density and electron energy density values, the pnicogen−N ylides being the strongest bonds; this behavior can also be found along the remaining series **b**, **c**, and **d** (also see the Supporting Information). From these results, we conclude that bonds with Y = N, compared with those with P and As, show higher electron enrichment.

An analysis of the results of Table 3 indicates that the presence of F substituents in these ylides, where X = N (**1a**, **4a**), significantly increases the electron energy density (more negative values), changing the nature of the bond. Me substitution (series **c** and **d**) also reinforced the central bond, but the changes are almost insignificant (see the Supporting Information, Table S-2).

Although we have seen that F presence reinforces the central X−Y bond (most significantly for **1a** and **4a**), the Laplacian apparently shows dissimilar values. The bond strengthening from **1a** to **1b** is clearly observed in the Laplacian values, **1b** showing a much more negative value. However, this is not the case for **4a** and **4b**, the latter presenting a positive value of 0.508, which can be explained in terms of the topology of the electron density (see the plots in Figure 1). In this figure, we can see that, after F introduction into compounds **4a** and **4b**, a huge charge-concentration zone is present in the middle of the X−Y bond. However, the interatomic surface (including the BCP) has been displaced toward the P atom, pushing the BCP inside the P charge-depleted shell, thus showing a more positive value. These results point out an increase of the central charge concentration; therefore, there is a bond strengthening and an increase of the covalent character in compound **4b**.

An analysis of the Laplacian reported in Table 3 shows a wide range of values for compounds of the same series: However, if we look at the electronegativity of the pnicogen atoms, we realize that, for the ylides where the X and Y atoms have similar electronegativity, the BCP is located in a charge-concentration zone, except for the ylides where Y = As. This can be explained by the very large charge-depletion zone in the outer shells of As (see the Laplacian plots in the Supporting Information).

Ellipticity is another property of the electron density that describes the anisotropy of the BCPs, and it can be related to the bond multiplicity. The ellipticity is defined as 1 minus the ratio between the most pronounced curvatures in $\rho(r)$, e.g., $\rho(r) = 1 - \lambda_1/\lambda_2$. For the ylides within the **a** series, the lowest values are those of the pnicogen−N ylides, while the pnicogen−P compounds lead to the highest values (0.5−0.7). The ellipticity for pnicogen−As is also high. This $\rho(r)$ property follows the same trends for the different substituents. As an indication of the bond multiplicity, ellipticity is expected to change with the presence of F next to X. Indeed this happens from the **a** to **b** series, except for **4b**, where the ellipticity is diminished from 0.722 to 0.466.

dx.doi.org/10.1021/jp204441p |*J. Phys. Chem. A* 2011, 115, 8316–8326

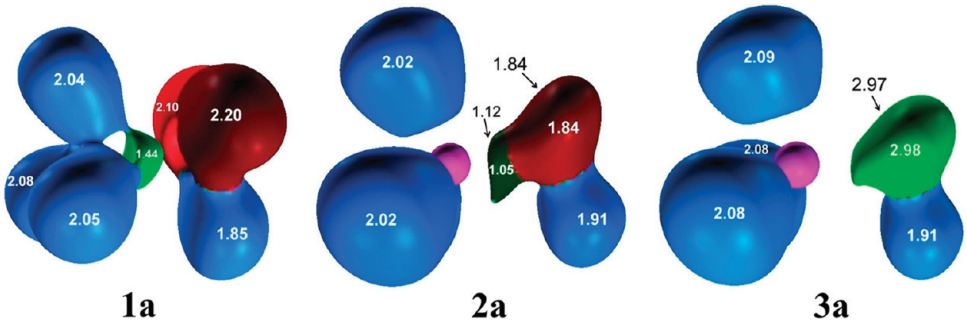

Figure 2. ELF representation at 0.7 for **1a**−**3a** at the MP2/6-311+G*//MP2/6-311+G* level.

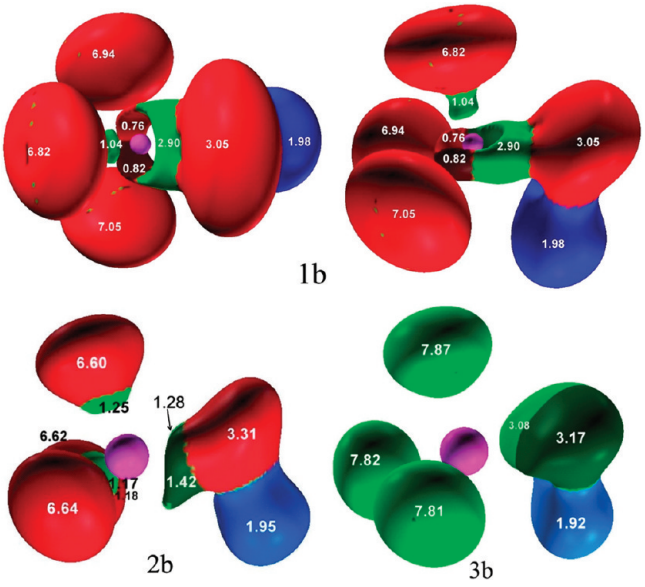

Figure 3. ELF representation at 0.7 for **1b**−**3b** at the MP2/6-311+G*//MP2/6-311+G* level (perpendicular and longitudinal points of view for **1b**).

This result is associated with the particular geometry, consisting of an almost planar distribution of all atoms except one of the F atoms. In the next section, the ELF analysis allows this behavior to be clarified. In accordance with the increment of both the ellipticity and delocalization index, which measures the electron exchange between two neighboring atomic basins, the presence of F increases the bond order. In addition, the QTAIM charges integrated into the X and Y basins have been calculated and reported in Table 3. Generally, the charge at the Y atoms is systematically reduced after the introduction of F.

3.1.3. ELF Analysis. Until now, we have had only partial information about the electronic arrangement in these compounds from the geometrical and QTAIM analyses. We have indications that some of the unsubstituted compounds seem to present ylidic character, noticed in no R−X bond differentiation, longer X−Y bond distances, and electron density details, while others already show indications of a more ylidene character, noticed in a higher bond multiplicity. After fluorine introduction, the situation changes, and those ylidic bonds show sharp geometric and electronic disturbances, while the other ones present a change toward bond strengthening, but no abrupt transition is noted. All of this will be clarified with the ELF analysis.

For the ELF analysis, here we show the graphs only for selected nonsubstituted and fluorinated compounds, the others being provided in the Supporting Information. There we can again see how the effects induced by CH_3 are reduced.

For nonsubstituted compounds, **1a** (see Figure 2), a prototypical bonding situation appears: there is a highly isotropic disynaptic basin between the two N atoms, which is very close to X, and this basin contains almost 2 electrons, this arrangement clearly corresponding to ylidic bonding character. Additionally, the presence of two highly populated monosynaptic basins next to the Y atom also supports this result.

However, the electronic arrangement changes drastically after introduction of F onto the X atom (**1b**) (see Figure 3). Now the central X−Y disynaptic basin changes in shape and population, having an almost toroidal arrangement around X, its population being almost 3 e^-. Additionally, if we compare monosynaptic basins next to the Y atom in **1a** and **1b**, we see that the number of basins is reduced together with the overall population of those basins (4.30 e^- for **1a** and 3.05 e^- for **1b**). This indicates a clear change in the electronic environment for Y and, together with the anisotropy of the central basin, supports the idea of ylidene character. ELF analysis allows us to find a clue for why there is one distinct F−X bond (the one that lies on the symmetry plane). This F atom shows a shorter bond length because of the presence of a small disynaptic basin that avoids the toroidal central basin mentioned above. On the other hand, the other F atoms have longer bonds due to the presence of a repulsion with the toroidal electronic arrangement around X. This arrangement provokes a different stability, and the F−X bond with a disynaptic basin is much more stable than the other ones (see the Supporting Information).

We have just seen a qualitative change in the bond nature after modification of the chemical environment around the bond. For the other compounds, these modifications would not have such drastic implications because the ylidene character was partially there. Thus, we can see how, for the nonsubstituted P−N ylide **2a**, a disynaptic basin is already present between P and N, although the N atom in the Y position still holds two monosynaptic basins. When we compare the ELF bonding schemes of **2a** and **1a**, we notice that the monosynaptic basin charge is shifted toward the central area, increasing the population of the central bond, this possibly being the cause of the topological change in the X−Y bond. For X = As compounds, this displacement is reinforced up to a total integration of the electron density in the central disynaptic basins (**3a**). This reveals a different behavior for N and the other pnicogen atoms, compound **2a** being the first one where the ylidene character can be detected, as indicated by the topological change in the ELF analysis.

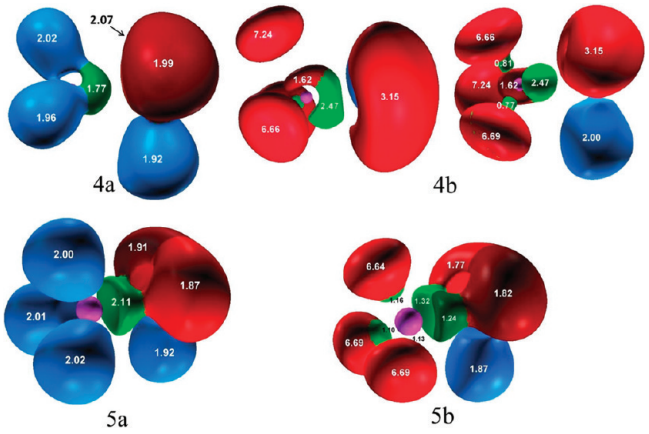

Figure 4. ELF representation at 0.7 for **4a,b** and **5a,b** at the MP2/6-311+G*//MP2/6-311+G* level (longitudinal and perpendicular points of view for **4b**).

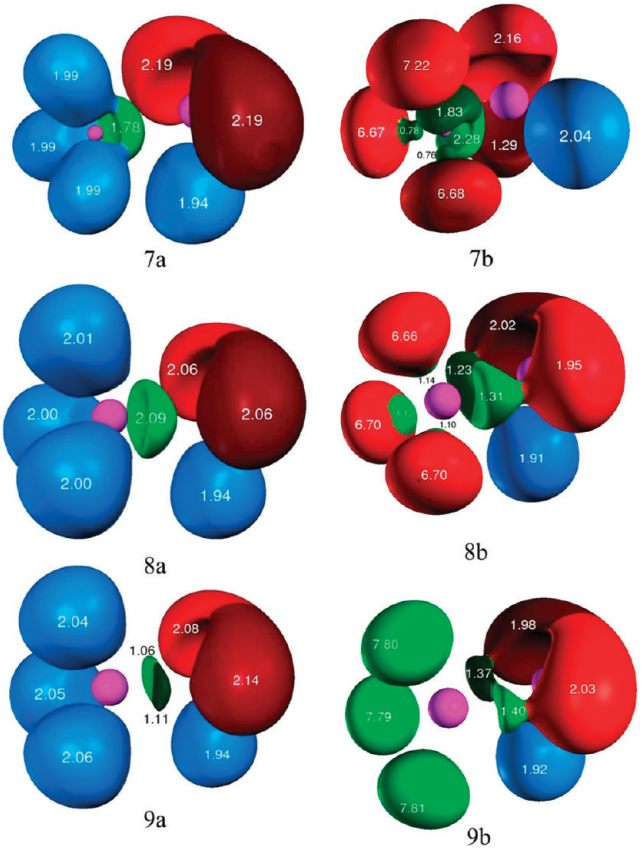

Figure 5. ELF representation at 0.7 for **7a**−**9a** and **7b**−**9b** at the MP2/6-311+G*//MP2/6-311+G* level.

After introduction of F, the bonding scheme will not be altered as much as it was before for N−pnicogen bonds, and the changes introduced will be far milder. We see how the basin shapes are similar for compounds **2a** and **3a**, although an increase of the central basin population for **2b** is accompanied by a reduction of the population of the monosynaptic basin next to Y (in this case only a monosynaptic basin next to Y appears). The bonding situations and ELF shapes in **3a** and **3b** are similar. In both cases, the presence of a F substituent does not yield a topological change, but an increase in the ylidene character can be sensed, as the double bond character already appeared in compounds **2a** and **3a**.

The pnicogen−P ylides follow the general trends described above. Compound **4a** (see Figure 4) has a typical ylidic character with two bulky basins in the Y atom (P) and only one disynaptic and isotropic basin in the central bond. Also, F presence in **4b** severely deforms the system, the central basin now showing high anisotropy, surrounding the N atom (X) in a fashion similar to that in **1b**. In these systems, the F−X bonds are differentiated for reasons similar to those in **1b**.

An analysis of the ELF is capable of explaining the unusual geometric arrangement for this system. Let us recall that all atoms except one F atom are located almost in the same plane, and because of the toroidal shape of the central basins in **4b**, the two atoms can form a covalent interaction with X, but only in the direction perpendicular to the toroidal central basin. This leads all atoms to share a molecular plane except the remaining F atom, which is weakly bonded. Another geometrical feature concerns the low τ values for compounds **4**−**9** for all series. The ELF plots reveal the huge volume of monosynaptic basins held by Y is responsible for the repulsion of the H bonded to Y. This situation does not take place in compounds **1**−**3**.

For both **5a** and **2a**, we can expect a similar behavior, and the central bond has an intermediate character between a double and a single bond. In **5a**, we notice a disynaptic basin shape very similar to that of **5b**, although only one attractor was found. However, the similarity in shape indicates that we are close to the appearance of two central basins. In this particular case, F causes the partition of the central basin, increasing the population in the central bond and slightly depopulating the monosynaptic basins. However, the introduced changes are not as remarkable as in **4a,b**.

Finally, analyzing the pnicogen−As compounds (Figure 5), we find that their behavior is similar to that of the pnicogen−P compounds: that is, the appearance of drastic changes from **7a** to **7b** and the reinforcement of the central bond multiplicity in the remaining ones. Also, as happened in pnicogen−P compounds, when X = P (**8a**), there is only one disynaptic central basin, but this time, the shape difference that arises after F addition is much more noticeable, not only in the division of the central basin but also in a substantial elongation of the shape of both basins together.

If we compare the entire series, we can conclude that, depending on the particular combination of X and Y atoms, the central bond may present a different bond nature, with different multiplicity. It seems quite clear that when X = N, the central bond can be interpreted mostly as an ylidic one, while when X = As, the bond shows a clear ylidene, double-bond character, as noticed in an elongated basin structure, often divided into two basins. However, a mixed situation appears when X = P. There the central bond seems to show a somewhat undefined behavior that varies with Y, indicating the intermediate character of these compounds (**2a**, **5a**, and **8a**).

From the results presented, we can conclude that both CH_3 and F substitutions at Y and X, respectively, induced a push−pull electron displacement (especially F) through the whole molecule from the Y to X atom that affects the nature of the central bond. The electron flow results in an enrichment of the region between X and Y, reinforcing the multiple character of that bond. The presence of a F substituent enhances the ylidene character, but in the case where X = N, this effect is not able to form a double bond (because of the lack of valence electrons) due to severe geometrical changes that allow the

dx.doi.org/10.1021/jp204441p |J. Phys. Chem. A 2011, 115, 8316–8326

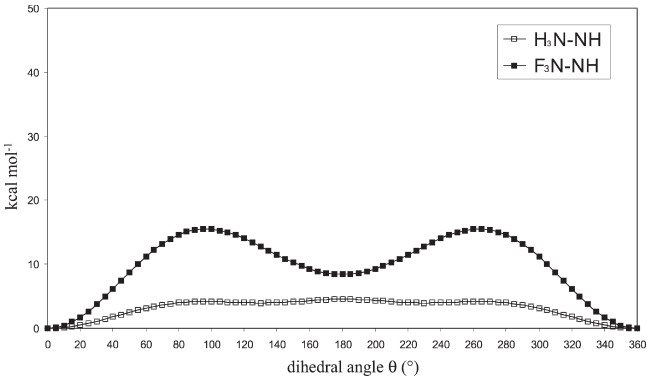

Figure 6. Rotational barriers for compounds **1a** and **1b** at the MP2/6-311++G**//MP2/6-311++G** level.

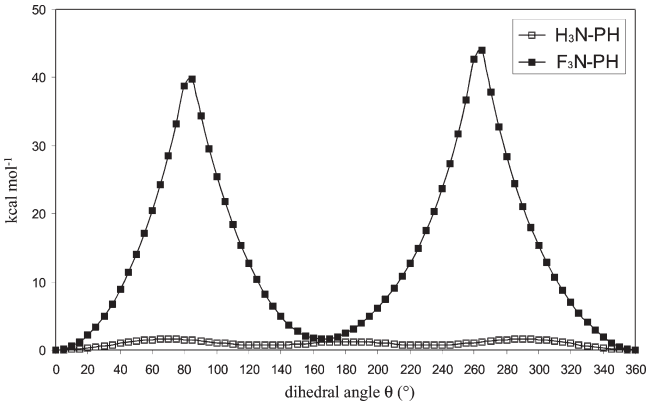

Figure 7. Rotational barriers for compounds **4a** and **4b** at the MP2/6-311++G**//MP2/6-311++G** level.

formation of a double bond, although resulting in a heavy differentiation of R−X bonds.

3.2.4. Rotational Barriers. Toward a deeper understanding of the bonding nature of these compounds, the rotational barriers around the X−Y bond have been studied. We can expect a relationship between energy and electronic properties. We performed only the scan for the **a** and **b** series, attending only to the compounds where the X atom is replaced by F. The barriers were a function of the R′−X−Y−H dihedral angle, θ. In all cases, the minimum was found at a dihedral angle of 180°. For the sake of clarity, we will discuss only the three distinct regions along the energy profiles. In addition, the remaining rotational barriers are presented in the Supporting Information.

One of these cases concerns the N−N ylides. When replaced by H, **1a**, the rotational profile is very low (below 5 kcal·mol^{-1}), indicating that the groups are free to rotate. The addition of a F substituent to this compound (**1b**) results in the appearance of two maxima (close to 20 kcal·mol^{-1}) due to the double-bond contribution induced by F (Figure 6). This is in agreement with the results derived from the ELF analysis. A rotation of the Y−H group yields a repulsion between double-bond basins and those from the X substituents in compound **1b**.

A similar situation, also characterized by a sudden appearance of the X−Y double bond, can be found in compounds **4a** and **4b**. The N−P bond in **4a** shows a clear single-bond profile with low values for the energy barrier. For this bond, the substitution of F

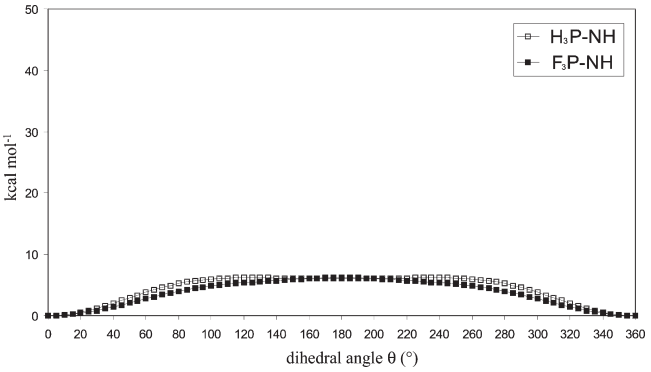

Figure 8. Rotational barriers for compounds **2a** and **2b** at the MP2/6-311++G**//MP2/6-311++G** level.

next to the N atom yields even more pronounced changes, showing two sharp maxima at 90° and 270° above 40 kcal·mol^{-1} (Figure 7). Again, this behavior can be explained in terms of the ELF analysis and the corresponding geometrical planar arrangement. The appearance of two maxima is caused by the repulsion of basins around N with those of F due to their strong repulsion situations, causing the presence of the maxima along the rotational barrier profiles.

However, for those ylides where Y = N (bonded to P and As), the rotational barriers remain unchanged after the substitution with F (Figure 8). This can be explained by means of the ELF analysis; in this case, the central basin is connected only with the Y lone pair basins while the rotation of the Y−H bond is free. Nevertheless, a small second-order effect is appreciable in the slight interaction between the central basin and the closest F basins. For those positions, where the fluorine basin is located closed to the central bond (at θ = 180°), a repulsive interactions is noticed, leading to the maximum in the rotational barrier.

3.2. Aza- and Arsa-Wittig Reactions. To obtain deeper insight into the nature of the ylidic bond and its associated chemical reactivity, we have studied a set of reactions involving aza- and arsa-Wittig rearrangements. The energy profiles calculated are depicted in Figure 9. For these reactions, two transition states and one intermediate, associated with a cyclic compound, are found. In addition, both QTAIM and ELF analyses have been performed at stationary points.

However, a clear idea about the origins of the different reactivities can be gained only by analyzing the electronic structure. Therefore, here we again analyze the AIM and ELF for the different transition states and intermediates in these reactions. This analysis will demonstrate the relevance of the ylidic bond nature in determining the reaction profile.

The main difference between the profiles of aza- and arsa-Wittig reactions lies in the presence of a higher stabilization of the intermediate compound for the aza-Wittig reaction (−21.0 kcal·mol^{-1} compared to −11.3 kcal·mol^{-1} for the arsa-Wittig intermediate). This happens not only for the intermediate, but also for the second transition state (TS2) and products. The three reaction paths present similar values of the relative energy among the different stationary points. This can be seen clearly in the similar energy difference between TS2 and the intermediates for both reactions (17.8 and 19.4 kcal·mol^{-1}).

A comparative analysis reveals that the whole reaction path can be divided into two main parts that behave differently: the first one is composed by reactants and TS1, and the second one

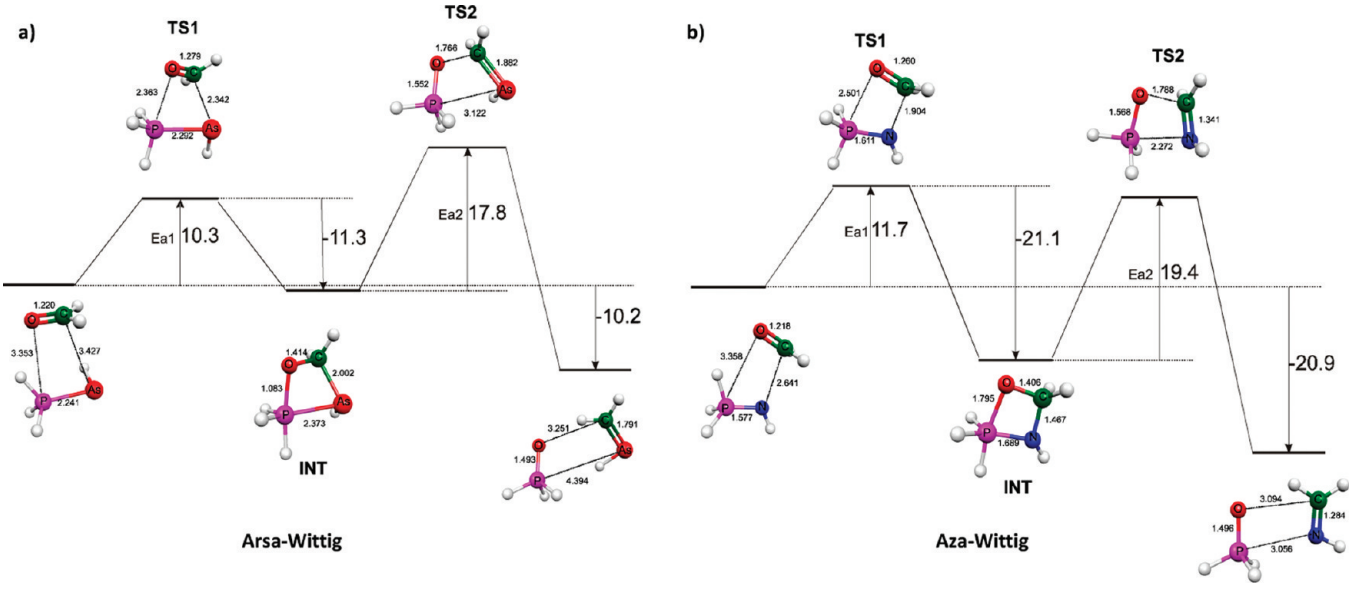

Figure 9. Energy profile (kcal·mol^{-1}) for the (a) arsa- and (b) aza-Wittig reactions.

Table 4. Geometric Properties and Electronic Properties for Central Bonds in Transition States and Intermediates, Electron Density at the Bond Critical Point $\rho(r_c)$ and Delocalization Index between the X and Y Basins δ(X,Y)

		bond lengths and angles (Å, deg)			$\rho(r_c)$ (e$^-$ a_0^{-3})			δ(X,Y)		
		TS1	INT	TS2	TS1	INT	TS2	TS1	INT	TS2
arsa-Wittig	P−As	2.292	2.373	3.122	0.093	0.091	0.022	0.84	0.74	0.12
	C−O	1.279	1.414	1.766	0.350	0.268	0.103	1.14	0.92	0.56
	As−C	2.342	2.002	1.882	0.070	0.127	0.143	0.54	0.86	1.20
	O−P	2.363	1.803	1.552	0.044	0.123	0.199	0.20	0.52	0.76
	P−As−C−O	42.1	22.0	−3.1						
	P−As−C−H	−80.6	−89.9	−88.4						
Aza-Wittig	P−N	1.611	1.689	2.272	0.200	0.171	0.061	0.90	0.68	0.30
	C−O	1.260	1.406	1.788	0.373	0.276	0.107	1.24	0.92	0.54
	N−C	1.904	1.467	1.341	0.086	0.258	0.345	0.46	0.92	1.30
	O−P	2.501	1.795	1.568	0.030	0.125	0.194	0.12	0.48	0.80
	P−N−C−O	10.4	10.5	−12.1						
	P−N−C−H	−143.1	−142.6	−107.6						

corresponds to the intermediate, TS2, and the products. When both reactions are compared, the second part of the energy profile for the aza-Wittig is lowered about 9 kcal·mol^{-1} with respect to the arsa-Wittig one. This can be explained in terms of enhanced stabilization of the reagent and TS1 in the arsa-Wittig reaction, with the help of the electronic structure analysis. This effect is the one that causes the aza-Wittig reaction to be more favorable.

From the geometrical standpoint (see Table 4), along the reaction pathway, the P−pnicogen and C−O bonds break while the pnicogen−C and P−O bonds form. This can be deduced from the values of the electron density and delocalization indices listed in Table 4.

However, in this process, differences arise according to the particular pnicogen used in each Wittig-type reaction. For TS1, different values of pnicogen−O distances can be sensed due to the different sizes of N and As atoms. Together with this effect, also a significant deformation (see the P−As−C−O dihedral angles) of the central ring can be appreciated for all stationary points of the energy profile for the arsa-Wittig reaction. If As is present in the central ring of the intermediate compound, the ring is puckered, but the intermediate for the aza-Wittig reaction shows an almost planar central ring. An additional effect is noticed in the axial arrangement of the H next to the As atom, this being placed almost perpendicularly to the average ring plane (see the P−As−C−H dihedral angles near to 90°). However, for the aza intermediate, the H bonded to N is closer to the ring plane.

Use of the electron-pairing structure, as resulted from the ELF analysis shown in Figure 10, provides us an explanation for the stabilization in the latter part of the aza-Wittig reaction (equivalent to a stabilization of the earlier part of the arsa-Wittig reaction). In the case of the As atom, two huge valence basins appear, while the equivalent basins for N are much closer to its

dx.doi.org/10.1021/jp204441p |J. Phys. Chem. A 2011, 115, 8316–8326

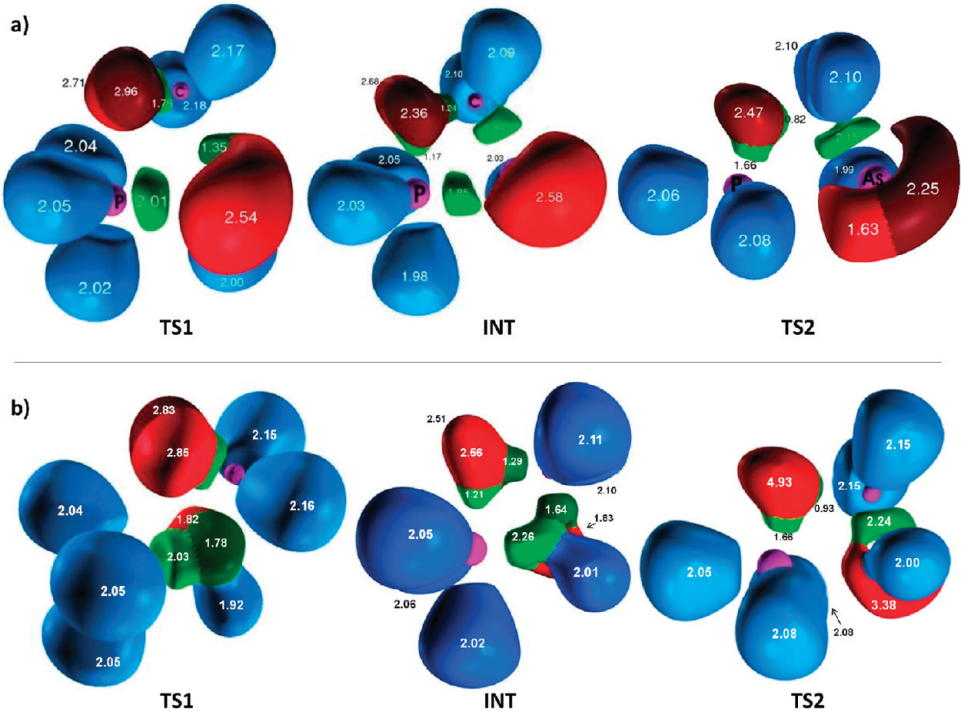

Figure 10. ELF representation for the first transition state, intermediate, and second transition state for the (a) arsa- and (b) aza-Wittig reactions.

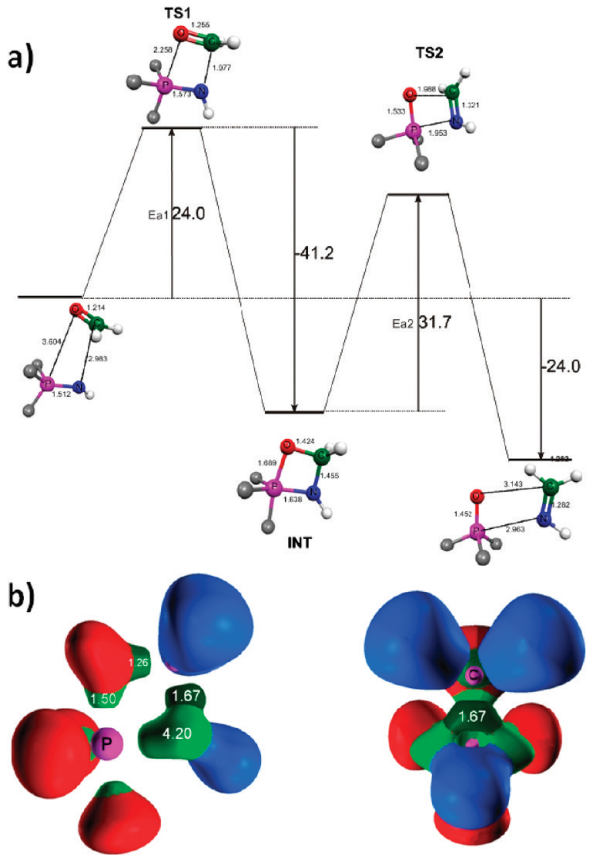

Figure 11. (a) Energy profile (kcal·mol^{-1}) for the aza-Wittig reaction with the fluorinated ylide. (b) Longitudinal and perpendicular point of view for the ELF representation of the intermediate.

corresponding core. After the initial stages of both reactions, the interaction between C and the pnicogen atom causes a differentiation of the previously symmetric basins (those that corresponded with the unpaired electrons) in both volume and population, with a volume reduction in one of them. However, only for the arsa-Wittig reaction is this reduction sharpest, even at the earliest stages of the reaction. This behavior may be associated with an incipient bonding between both C and As atoms due to high electron pairing between them (a disynaptic basin). Energetically, there is a stabilization of the initial stages of the reaction, which explains the shifting of the first two stages of the arsa-Wittig reaction when compared to the aza-Wittig reaction.

This interaction yields an additional effect: the high lobe differentiation for As results also in having C attached to one side of the ylide, while in the case of N, the equivalent basins are so near that the C atom can be placed directly over the N atom. This is directly related to the ring shape in the intermediates. Bonding with As provokes a wide separation between the two As valence basins, forcing the C atom to stay away from the molecular plane, and a twisting of the central ring takes place. This causes the deformation of the central ring for the arsa-Wittig reactions.

The axial disposition of the H atom for the intermediate compound of the arsa-Wittig reaction can be explained by the great volume of the remaining As monosynaptic valence basin (the one that did not participate in the construction of the As−C bond). This basin pushes the H atom away from the ring plane, forcing H, As, and its monosynaptic basin to be aligned. This does not happen with N, because all basins are close to the N core, the repulsion thus being much lower.

In an effort to understand the changes induced in the reactivity by the substitution with fluorine, the aza-Wittig reaction has been reported with compound **2b** to evaluate the electron push effect of F (Figure 11). With this ylide, the reaction profile changes substantially; the presence of F results in higher barriers for both

transition states, while the intermediate is even more stabilized. Also, these results can be explained in terms of electron density arrangement. If we study the ELF representation for the intermediate, we note that the unshared basin that belongs to the pnicogen atom has vanished, and now we see a huge toroidal disynaptic basin between the P and N atoms, with a population of 4.20 e^-. As a consequence, this intermediate has a planar structure (H being attached to N contained in the molecular plane). Such electron arrangement results in a large stabilization of the intermediate molecular system. At this point, we need to bear in mind the results found in the previous part of this work, where F reinforced the central ylide bond. Both results help explain the high barriers that resulted in this reaction, because the reaction pathway from stabilized reactants to intermediate requires an additional energy cost for the bond cleavage.

4. CONCLUSIONS

By using the topological analysis of the electron density, derived from QTAIM and ELF methods, the N, P, and As ylides and aza- and arsa-Wittig reactions were studied. Calculations were performed at the MP2/6-311++G** and B3LYP/6-311++G** levels to find an adequate description of their geometric, energetic, and electronic characteristics. The main conclusions can be summarized as follows:

(i) Depending on the pnicogen atom at the Y position, the pnicogen−pnicogen ylides show different behavior. For P and As derivatives, the bonds yield mainly a mild double-bond contribution, while for the N ylides, single-bond characteristics are evident.

(ii) The F substituents consistently reinforce the central bond, this being noticed in a bond shortening and in an increase of the electron population, leading invariably to a double-bond situation, even for the N ylides.

(iii) Due to the limitation for N atoms to form four covalent bonds, one of the F interactions with the N atom becomes different, being characterized as a clear electrostatic interaction, with larger bond distances and absence of disynaptic basins.

(iv) Arsa- and aza-Wittig reactions proceed by a two-step mechanism with a stable cyclic intermediate. From a thermodynamic point of view, the arsa-Wittig rearrangement is less exothermic than the aza-Wittig rearrangement. This difference can be associated with the stabilization of the first stage for the arsa-Wittig reaction, caused by an early development of the As−C bond.

(v) The size of the pnicogen in the Y position determines the particular geometric arrangement during the reactions. For bigger pnicogen atoms such as As, a puckering of the central ring and a different orientation of the H substituent are noted. These effects can be understood by the larger volume and separation of As valence basins, which allow the early formation of the As−C bond, but also cause C to be attached laterally to the ylide, pushing the H substituent toward an axial conformation.

(vi) Substitution with electronegative groups (explored here with F atoms) generally improves the electron localization, stabilizing the structure and yielding higher bond orders.

(vii) Along the Wittig-type reactions, F substitution strengthens and stabilizes of the reactants, products, and intermediates, and therefore, larger values of the energy barrier are found throughout the energy profiles.

■ ASSOCIATED CONTENT

Supporting Information. Geometrical parameters (Table S-1), electronic properties for X−Y bonds (Table S-2), Laplacian plots of the electron density (Figures S-3−S-5), ELF representations (Figures S-6−S-9), and rotational barriers (Figures S-10−S-16). This material is available free of charge via the Internet at http://pubs.acs.org.

■ AUTHOR INFORMATION

Corresponding Author
*E-mail: dobado@ugr.es.

■ ACKNOWLEDGMENT

This work was financed by the Ministerio de Ciencia y Tecnología, Grant BQU2002-01207. We thank the Centro de Servicios de Informática y Redes de Comunicaciones (CSIRC), Universidad de Granada, for the computational resources (UGRGrid). Mr. David Nesbitt reviewed the English version of the manuscript.

■ REFERENCES

(1) Pailer, M.; Haslinguer, E. *Monatsh. Chem.* **1970**, *101*, 508–511.
(2) Kloek, J. A.; Leschinsky, K. L. *J. Org. Chem.* **1978**, *43*, 1460–11462.
(3) Heffe, W. Ph.D. Dissertation, University of Berlin, 1937, quoted by G. Wittig: *Pure Appl. Chem.* **1964**, *9*, 245−254.
(4) Raeck, C.; Berger, S. *Eur. J. Org. Chem.* **2006**, *21*, 4934–4937.
(5) Smith, R. C.; Gantzel, P.; Rheinhold, A. L.; Protasiewicz, J. D. *Organometallics* **2004**, *23*, 5124–5126.
(6) Huang, Z.-Z.; Huang, X.; Huang, Y.-Z. *J. Chem. Soc., Perkin Trans. 1* **1995**, 95–96.
(7) Starzewski, K. A. O.; Dieck, H. T. *Inorg. Chem.* **1979**, *18*, 3307–3316.
(8) Sudhakar, P. V.; Lammertsma, K. *J. Am. Chem. Soc.* **1991**, *113*, 1899–1906.
(9) Lu, W. C.; Sun, C. C. *THEOCHEM* **2002**, *593*, 1–7.
(10) Molina, P.; Alajarin, M.; Lopez-Leonardo, C.; Claramunt, R. M.; Foces-Foces, M. C.; Hernandez-Cano, F.; Catalan, J.; De Paz, J. L. G.; Elguero, J. *J. Am. Chem. Soc.* **1989**, *111*, 355–363.
(11) Koppel, I. A.; Schwesinger, R.; Breuer, T.; Burk, P.; Herodes, K.; Koppel, I.; Leito, I.; Mishima, M. *J. Phys. Chem. A.* **2001**, *105*, 9575–9586.
(12) Rak, J.; Skurski, P.; Liwo, A.; B-lazejowski, J. *J. Am. Chem. Soc.* **1995**, *117*, 2638–2648.
(13) Skurski, P.; Gutowski, M.; Simons, J. *J. Chem. Phys.* **1999**, *110*, 274–280.
(14) Bader, R. F. W. *Atoms in Molecules: A Quantum Theory*; Clarendon Press: Oxford, U.K., 1990.
(15) Bader, R. F. W. *Chem. Rev.* **1991**, *91*, 893–928.
(16) Bader, R. F. W. In *Encyclopedia of Computational Chemistry*; Schleyer, P. v. R., Ed.; Wiley: Chichester, U.K., 1998.
(17) Becke, A. D.; Edgecombe, K. E. *J. Chem. Phys.* **1990**, *92*, 5397–5403.
(18) Silvi, B.; Savin, A. *Nature* **1994**, *371*, 683–686.
(19) Silvi, B.; Fourré, I.; Alikhani, M. E. *Monatsh. Chem.* **2005**, *136*, 855–879.
(20) Silvi, B. *Phys. Chem. Chem. Phys.* **2004**, *6*, 256–260.
(21) Molina, P; Vilaplana, M. J. *Synthesis* **1994**, *218*, 1197–1218.
(22) Cossío, F. P.; Alonso, C.; Lecea, B.; Ayerbe, M.; Rubiales, G.; Palacios, F. *J. Org. Chem.* **2006**, *71*, 2839–2847.
(23) Xue, Y.; Xie, D.; Yan, G. *J. Phys. Chem. A* **2002**, *106*, 9053–9058.
(24) Koketsu, J.; Ninomiya, Y.; Suzuki, Y.; Koga, N. *Inorg. Chem.* **1997**, *36*, 694–702.

(25) Lu, W. C.; Sun, C. C.; Zang, Q. J.; Liu, C. B. *Chem. Phys. Lett.* **1999**, *311*, 491–498.
(26) Lu, W. C.; Zhang, R. Q.; Zang, Q. J.; Wong, N. B. *J. Phys. Chem. B* **2003**, *107*, 2061–2067.
(27) He, H. S.; Chung, C. W. Y.; But, T. Y. S.; Toy, P. H. *Tetrahedron* **2005**, *61*, 1385–1405.
(28) Møller, C.; Plesset, M. S. *Phys. Rev.* **1934**, *46*, 618–622.
(29) Becke, A. D. *J. Chem. Phys.* **1993**, *98*, 5648–5652.
(30) Frisch, M. J.; Trucks, G. W.; Schlegel, H. B.; Scuseria, G. E.; Robb, M. A.; Cheeseman, J. R.; Montgomery, J. A., Jr.; Vreven, T.; Kudin, K. N.; Burant, J. C.; Millam, J. M.; Iyengar, S. S.; Tomasi, J.; Barone, V.; Mennucci, B.; Cossi, M.; Scalmani, G.; Rega, N.; Petersson, G. A.; Nakatsuji, H.; Hada, M.; Ehara, M.; Toyota, K.; Fukuda, R.; Hasegawa, J.; Ishida, M.; Nakajima, T.; Honda, Y.; Kitao, O.; Nakai, H.; Klene, M.; Li, X.; Knox, J. E.; Hratchian, H. P.; Cross, J. B.; Bakken, V.; Adamo, C.; Jaramillo, J.; Gomperts, R.; Stratmann, R. E.; Yazyev, O.; Austin, A. J.; Cammi, R.; Pomelli, C.; Ochterski, J. W.; Ayala, P. Y.; Morokuma, K.; Voth, G. A.; Salvador, P.; Dannenberg, J. J.; Zakrzewski, V. G.; Dapprich, S.; Daniels, A. D.; Strain, M. C.; Farkas, O.; Malick, D. K.; Rabuck, A. D.; Raghavachari, K.; Foresman, J. B.; Ortiz, J. V.; Cui, Q.; Baboul, A. G.; Clifford, S.; Cioslowski, J.; Stefanov, B. B.; Liu, G.; Liashenko, A.; Piskorz, P.; Komaromi, I.; Martin, R. L.; Fox, D. J.; Keith, T.; Al-Laham, M. A.; Peng, C. Y.; Nanayakkara, A.; Challacombe, M.; Gill, P. M. W.; Johnson, B.; Chen, W.; Wong, M. W.; Gonzalez, C.; Pople, J. A. *Gaussian 03*, revision B.05; Gaussian, Inc.: Pittsburgh, PA, 2003.
(31) Noury, S.; Krokidis, X.; Fuster, F.; Silvi, B. *Comput. Chem.* **1999**, *23*, 597–604.
(32) MORPHY98, a program written by P. L. A. Popelier with a contribution from R. G. A. Bone, University of Manchester Institute of Science and Technology, Manchester, U.K., 1998.
(33) Popelier, P. L. A. *Comput. Phys. Commun.* **1996**, *93*, 212–240.
(34) Popelier, P. L. A. *Chem. Phys. Lett.* **1994**, *228*, 160–164.
(35) Biegler-König, F.; Schönbohm, J.; Bayles, D. *J. Comput. Chem.* **2001**, *22*, 545–559.
(36) Pepcke, E.; Lyons, J. *SciAn 1.2*; Supercomputer Computations Research Institute, Florida State University: Tallahassee, FL, 1996.
(37) Synaptic order is defined for a valence basin as the number of connections with core basins.